arXiv:1609.05828v1 [math.NA] 19 Sep 2016

P_1-nonconforming divergence-free finite element method on square meshes for Stokes equations

Chunjae Park *

Tuesday 20th September, 2016

Abstract

Recently, the P_1-nonconforming finite element space over square meshes has been proved stable to solve Stokes equations with the piecewise constant space for velocity and pressure, respectively. In this paper, we will introduce its locally divergence-free subspace to solve the elliptic problem for the velocity only decoupled from the Stokes equation. The concerning system of linear equations is much smaller compared to the Stokes equations. Furthermore, it is split into two smaller ones. After solving the velocity first, the pressure in the Stokes problem can be obtained by an explicit method very rapidly.

1 Introduction

A divergence-free vector field frequently appears in various mathematical and engineering problems such as an incompressible flow in the Navier-Stokes equation or a solenoidal magnetic induction in the Maxwell equations or the limit of displacements in elasticity equations when Poisson's ratio goes to 1/2.

An incompressible Stokes problem can be reduced to an elliptic problem for the velocity only in the divergence-free space [5]. The locally divergence-free subspace of $[\mathcal{CR}]^2$ was used for finite element methods to solve that elliptic problem [2, 13], where $\mathcal{CR}$ is the Crouzeix-Raviart P_1-nonconforming finite element space on triangular meshes. It have also been adopted for the time-harmonic Maxwell equations [1].

It is equipped with sufficient interpolants for continuous divergence-free functions in $[H^2]^2$, since it can be interpreted as the curls of the Morley element. If the domain is simply connected in $\mathbb{R}^2$, its dimension is the number of interior vertices and edges [6, 13], which is about two third of that of $[\mathcal{CR}]^2$.

A conforming locally divergence-free space whose elements are piecewise linear can be constructed with the curls of C^1-Powell-Sabin elements on triangular meshes for biharmonic problems [12]. Instead of working with divergence-free spaces, some researchers have developed finite element methods for Stokes equations whose velocity solutions are resulted divergence-free [8, 14] as well as locally divergence-free discontinuous Galerkin methods [3, 4].

In this paper, we are interested in the locally divergence-free subspace of $[\mathcal{NC}]^2$, the P_1-nonconforming finite element space on square meshes. The space $\mathcal{NC}$ consists of functions which are linear in each square and continuous on each midpoint of edge [10, 11]. Recently,

*Department of Mathematics, Konkuk University, Seoul 143-701, Korea, Emails: cjpark@konkuk.ac.kr

it has been proved that $[\mathcal{NC}]^2$ is stable to solve Stokes equations with the piecewise constant space for velocity and pressure, respectively [9].

We will apply the locally divergence-free subspace to solve the elliptic problem for the velocity only, reduced from the incompressible Stokes problem. The concerning system of linear equations is much smaller than that of the Stokes equation. Furthermore, it is split into two smaller ones for the red and black squares. After solving the velocity first, the pressure in the Stokes problem will be obtained by an explicit method very rapidly.

The paper is organized as follows. In the next section the P_1-nonconforming finite element space on quadrilateral meshes will be briefly reviewed. Then, restricted on square meshes, we will devote section 3 to characterizing its locally divergence-free subspace as well as a basis. In section 4, the reduced elliptic problem for the velocity and an explicit method for the pressure in the Stokes problem are stated, respectively. Finally, some numerical tests will be presented in the last section.

Throughout the paper, C_S is a generic notation for a constant which depends only on S.

2 P_1-nonconforming quadrilateral finite element

Let Ω be a simply connected polygonal domain in $\mathbb{R}^2$ with a triangulation $\mathcal{T}_h$ which consists of uniform squares of width and height h as in Figure 1. For a vertex or edge in $\mathcal{T}_h$, we call them a boundary vertex or edge if they belong to $\partial\Omega$, otherwise, an interior vertex or edge.

The P_1-nonconforming quadrilateral finite element spaces [10, 11] are defined by

$$\begin{aligned}\mathcal{NC}^h(\Omega) = \{v_h \in L^2(\Omega) \ : \ & v_h|_Q \in <1, x, y> \text{ for all squares } Q \in \mathcal{T}_h, \\ & v_h \text{ is continuous at every midpoints of edges in } \mathcal{T}_h\},\end{aligned}$$

$$\mathcal{NC}_0^h(\Omega) = \{v_h \in \mathcal{NC}^h(\Omega) \ : \ v_h(m) = 0 \text{ for all midpoints } m \text{ of boundary edges in } \mathcal{T}_h\}.$$

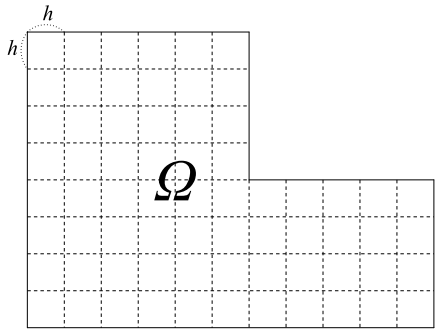

Figure 1: Triangulation $\mathcal{T}_h$ of $\overline{\Omega}$ into uniform squares

When we assign a value c_m for the midpoint m of each edge in $\mathcal{T}_h$, there exists $v_h \in \mathcal{NC}^h(\Omega)$ such that $v_h(m) = c_m$ at all midpoints m of edges in $\mathcal{T}_h$ if and only if

$$c_{m_1} + c_{m_3} = c_{m_2} + c_{m_4}, \tag{1}$$

whenever $m_1, \cdots, m_4$ are of clockwisely numbered edges of a square $Q \in \mathcal{T}_h$.

For each vertex $\mathbf{V}$ in $\mathcal{T}_h$, define a function $\psi^{\mathbf{V}} \in \mathcal{NC}^h(\Omega)$ by its values at all midpoints m of edges in $\mathcal{T}_h$ such that

$$\psi^{\mathbf{V}}(m) = \begin{cases} 1, & \text{if } m \text{ belongs to an edge which meets } \mathbf{V}, \\ 0, & \text{otherwise.} \end{cases} \tag{2}$$

Note $\psi^{\mathbf{V}} \in \mathcal{NC}^h(\Omega)$ is well defined since its values at the midpoints satisfy the condition (1). Then, we have a basis for $\mathcal{NC}_0^h(\Omega)$ as

$$\mathcal{NC}_0^h(\Omega) = \mathrm{Span}\{\psi^{\mathbf{V}} \in \mathcal{NC}_0^h(\Omega) \ : \ \mathbf{V} \text{ is an interior vertex in } \mathcal{T}_h\}. \tag{3}$$

Hence, the dimension of $\mathcal{NC}_0^h(\Omega)$ is the number of interior vertices in $\mathcal{T}_h$.

Define an interpolation $\pi_h : H_0^1(\Omega) \cap C(\Omega) \to \mathcal{NC}_0^h(\Omega)$ as

$$\pi_h v = \sum_{\mathbf{V}} \frac{v(\mathbf{V})}{2} \psi^{\mathbf{V}}, \quad \forall v \in H_0^1(\Omega) \cap C(\Omega), \tag{4}$$

where the summation runs over all interior vertices $\mathbf{V}$ in $\mathcal{T}_h$. We note $\pi_h v$ satisfies

$$\pi_h v\Big(\frac{\mathbf{V}_1 + \mathbf{V}_2}{2}\Big) \ = \ \frac{v(\mathbf{V}_1) + v(\mathbf{V}_2)}{2} \quad \text{for all adjacent vertices } \mathbf{V}_1, \mathbf{V}_2 \text{ in } \mathcal{T}_h. \tag{5}$$

Then, the interpolation error is estimated by

$$\|v - \pi_h v\|_{L^2(\Omega)} + h|v - \pi_h v|_{1,h} \ \le \ C_\Omega \, h^2 |v|_{H^2(\Omega)}, \quad \forall v \in H_0^1(\Omega) \cap H^2(\Omega),$$

where $|\Box|_{1,h}$ denotes the mesh-dependent discrete H^1-seminorm such that

$$|\Box|_{1,h} = \left[\sum_{Q \in \mathcal{T}_h} \int_Q |\nabla \Box|^2 \, dxdy \right]^{1/2}. \tag{6}$$

Let $\mathcal{Q}_{1,h}(\Omega)$ be the conforming piecewise bilinear space over $\mathcal{T}_h$ as

$$\mathcal{Q}_{1,h}(\Omega) = \{w_h \in H_0^1(\Omega) \cap C(\Omega) \ : \ w_h|_Q \in < 1, x, y, xy > \text{ for all squares } Q \in \mathcal{T}_h\},$$

with an assumption that $\partial\Omega$ consists of segments parallel to x, y-axes. Two lowest order finite element spaces $\mathcal{Q}_{1,h}(\Omega)$ and $\mathcal{NC}_0^h(\Omega)$ are isomorphic as in the following lemma.

Lemma 2.1. *Let $\pi_h : \mathcal{Q}_{1,h}(\Omega) \to \mathcal{NC}_0^h(\Omega)$ be the operator as in (4). Then π_h is a bijection.*

Proof. Let $\pi_h \in \mathcal{NC}_0^h(\Omega)$ vanish at all midpoints of edges in $\mathcal{T}_h$ for some $v \in \mathcal{Q}_{1,h}(\Omega)$. Then, v vanishes on each interior edges E in $\mathcal{T}_h$ which meets $\partial\Omega$, since v is linear on E and vanishes at the two endpoints of E by (5).

By sweeping out argument, v does on all edges in $\mathcal{T}_h$. It means that π_h is a bijection since the dimensions of $\mathcal{Q}_{1,h}(\Omega)$ and $\mathcal{NC}_0^h(\Omega)$ are same as the number of interior vertices in $\mathcal{T}_h$. □

For a vector valued function $\mathbf{v} = (v_1, v_2)$, the component-wise interpolation and discrete H^1-seminorm from (4) and (6) will be used as

$$\Pi_h \mathbf{v} = (\pi_h v_1, \pi_h v_2), \quad |\mathbf{v}|_{1,h} = \Big(|v_1|_{1,h}^2 + |v_2|_{1,h}^2\Big)^{1/2}.$$

Let $\mathrm{div}_h\,, \mathrm{curl}_h$ be the mesh-dependent discrete divergence and curl as

$$(\mathrm{div}_h\,\mathbf{v})\big|_Q = \mathrm{div}\,(\mathbf{v}|_Q), \quad (\mathrm{curl}_h\,\mathbf{v})\big|_Q = \mathrm{curl}\,(\mathbf{v}|_Q), \quad \forall Q \in \mathcal{T}_h.$$

It is well known there is a constant C_Ω such that [5]

$$|\mathbf{v}|_{[H^1(\Omega)]^2} \le C_\Omega(\|\mathrm{div}\,\mathbf{v}\|_{L^2(\Omega)} + \|\mathrm{curl}\,\mathbf{v}\|_{L^2(\Omega)}), \quad \forall \mathbf{v} \in [H_0^1(\Omega)]^2. \tag{7}$$

We have a similar result to (7) for $[\mathcal{NC}_0^h(\Omega)]^2$ in the following lemma.

Lemma 2.2. *For all $\mathbf{v}_h \in [\mathcal{NC}_0^h(\Omega)]^2$, we have*

$$|\mathbf{v}_h|_{1,h}^2 = \|\mathrm{div}_h\,\mathbf{v}_h\|_{L^2(\Omega)}^2 + \|\mathrm{curl}_h\,\mathbf{v}_h\|_{L^2(\Omega)}^2.$$

Proof. For each $\mathbf{w}_h = (w_1, w_2) \in [\mathcal{Q}_{1,h}(\Omega)]^2$, we have, by integration by parts,

$$\begin{aligned}\int_\Omega w_{1x}w_{2y}\,dxdy &= \sum_{Q\in\mathcal{T}_h}\int_Q w_{1x}w_{2y}\,dxdy \\ &= \sum_{Q\in\mathcal{T}_h}\int_{\partial Q} w_{1x}w_2\nu_y\,ds - \int_Q w_{1xy}w_2\,dxdy = -\sum_{Q\in\mathcal{T}_h}\int_Q w_{1xy}w_2\,dxdy,\end{aligned}$$

since ν_y is nonzero only at the horizontal edges of ∂Q and w_{1x}, w_2 are continuous there. The same argument is repeated to get

$$\begin{aligned}\int_\Omega w_{1y}w_{2x}\,dxdy &= \sum_{Q\in\mathcal{T}_h}\int_{\partial Q} w_{1y}w_2\nu_x\,ds - \int_Q w_{1yx}w_2\,dxdy \\ &= -\sum_{Q\in\mathcal{T}_h}\int_Q w_{1yx}w_2\,dxdy = \int_\Omega w_{1x}w_{2y}\,dxdy.\end{aligned} \tag{8}$$

Then, from (8), we can establish

$$\begin{aligned}|\mathbf{w}_h|_{[H^1(\Omega)]^2}^2 &= (w_{1x}, w_{1x}) + (w_{1y}, w_{1y}) + (w_{2x}, w_{2x}) + (w_{2y}, w_{2y}) \\ &= (w_{1x} + w_{2y}, w_{1x} + w_{2y}) + (w_{2x} - w_{1y}, w_{2x} - w_{1y}) \\ &= \|\mathrm{div}\,\mathbf{w}_h\|_{L^2(\Omega)}^2 + \|\mathrm{curl}\,\mathbf{w}_h\|_{L^2(\Omega)}^2.\end{aligned} \tag{9}$$

Now, if $\mathbf{v}_h = (v_1, v_2) \in [\mathcal{NC}_0^h(\Omega)]^2$, there exists $\mathbf{w}_h = (w_1, w_2) \in [\mathcal{Q}_{1,h}(\Omega)]^2$ by Lemma 2.1 such that

$$v_i = \pi_h w_i, \quad i = 1, 2.$$

Given square $Q \in \mathcal{T}_h$, assume that

$$w_i(x, y) = \alpha_i + \beta_i\hat{x} + \gamma_i\hat{y} + \delta_i\hat{x}\hat{y}, \quad i = 1, 2, \tag{10}$$

where $\hat{x} = x - c_1,\ \hat{y} = y - c_2$ for the center point (c_1, c_2) of Q. Note

$$\int_Q \hat{x}\,dxdy = \int_Q \hat{y}\,dxdy = \int_Q \hat{x}\hat{y}\,dxdy = 0. \tag{11}$$

By (5), $\pi_h \hat{x}\hat{y}$ vanishes at all midpoints of edges in $\mathcal{T}_h$ since the values of $\hat{x}\hat{y}$ differ only by their signs at every two endpoints of an edge of Q. It means v_i is the linear part of w_i so that

$$v_i(x,y) = \pi_h w_i(x,y) = \alpha_i + \beta_i \hat{x} + \gamma_i \hat{y}, \quad i = 1,2. \tag{12}$$

From (10), (11), (12), we expand that

$$\begin{aligned}
&|\mathbf{w}_h|^2_{[H^1(Q)]^2} - \|\mathrm{div}\, \mathbf{w}_h\|^2_{L^2(Q)} - \|\mathrm{curl}\, \mathbf{w}_h\|^2_{L^2(Q)} \\
&\quad = \int_Q (\beta_1 + \delta_1 \hat{y})^2 + (\gamma_1 + \delta_1 \hat{x})^2 + (\beta_2 + \delta_2 \hat{y})^2 + (\gamma_2 + \delta_2 \hat{x})^2 \, dxdy \\
&\qquad - \int_Q (\beta_1 + \delta_1 \hat{y} + \gamma_2 + \delta_2 \hat{x})^2 + (\beta_2 + \delta_2 \hat{y} - \gamma_1 - \delta_1 \hat{x})^2 \, dxdy \\
&\quad = \int_Q \beta_1^2 + \gamma_1^2 + \beta_2^2 + \gamma_2^2 - (\beta_1 + \gamma_2)^2 - (\beta_2 - \gamma_1)^2 \, dxdy \\
&\quad = |\mathbf{v}_h|^2_{[H^1(Q)]^2} - \|\mathrm{div}\, \mathbf{v}_h\|^2_{L^2(Q)} - \|\mathrm{curl}\, \mathbf{v}_h\|^2_{L^2(Q)}.
\end{aligned}$$

It completes the proof, since $\mathbf{w}_h$ satisfies (9). □

3 P_1- nonconforming divergence-free space

Let V_h be a locally divergence-free subspace of $[\mathcal{NC}_0^h(\Omega)]^2$ as

$$V_h = \{\mathbf{v}_h \in [\mathcal{NC}_0^h(\Omega)]^2 \ : \ \mathrm{div}_h\, \mathbf{v}_h = 0\}. \tag{13}$$

Throughout the remaining of the paper, in order to exclude a pathological triangulation $\mathcal{T}_h$ such as a ladder or a union of two rectangles whose intersection is merely one square or edge in $\mathcal{T}_h$, we assume that

Assumption 3.1. *No square has 4 boundary vertices. No interior edge meets 2 boundary vertices. If a square has only two boundary vertices, they are two endpoints of an edge.*

Let $\mathcal{P}_{0,h}(\Omega)$ be a space of piecewise constant functions as

$$\mathcal{P}_{0,h}(\Omega) = \{q_h \in L^2(\Omega) \ : \ q_h|_Q =< 1 > \text{ for all } Q \in \mathcal{T}_h\}.$$

The value of a function $q_h \in \mathcal{P}_{0,h}(\Omega)$ at a square $Q \in \mathcal{T}_h$ will be abbreviated to $q_h(Q)$.

For an interior vertex $\mathbf{V}$, let Q_1, Q_2, Q_3, Q_4 be the squares in $\mathcal{T}_h$ which meet $\mathbf{V}$, counterclockwisely numbered from the square whose left bottom vertex is $\mathbf{V}$ as in Figure 2-(a). Using the scalar basis function $\psi^{\mathbf{V}} \in \mathcal{NC}_0^h(\Omega)$ in (2), for a vector value (a,b), define a function $\psi^{\mathbf{V}}[a,b] \in [\mathcal{NC}_0^h(\Omega)]^2$ by its values at all midpoints m of edges in $\mathcal{T}_h$ such that

$$\psi^{\mathbf{V}}[a,b](m) = \begin{cases} (a,b), & \text{if } m \text{ belongs to an edge which meets } \mathbf{V}, \\ (0,0), & \text{otherwise.} \end{cases}$$

We can easily check that $\mathrm{div}_h\, \psi^{\mathbf{V}}[a,b],\ \mathrm{curl}_h\, \psi^{\mathbf{V}}[a,b] \in \mathcal{P}_{0,h}(\Omega)$ have nontrivial values at only 4 squares in $\mathcal{T}_h$, given as in Figure 2-(b), (c),

$$\mathrm{div}_h\, \psi^{\mathbf{V}}[a,b](Q_j) = \begin{cases} -(a+b)/h & \text{if } j = 1, \\ (a-b)/h & \text{if } j = 2, \\ (a+b)/h & \text{if } j = 3, \\ (b-a)/h & \text{if } j = 4, \end{cases} \tag{14}$$

$$\operatorname{curl}_h \psi^{\mathbf{V}}[a,b](Q_j) = \begin{cases} (a-b)/h & \text{if } j=1, \\ (a+b)/h & \text{if } j=2, \\ (b-a)/h & \text{if } j=3, \\ -(a+b)/h & \text{if } j=4. \end{cases} \tag{15}$$

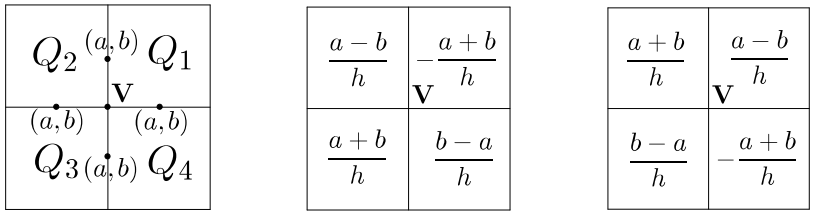

(a) $\psi^{\mathbf{V}}[a,b]$ (b) $\operatorname{div}_h \psi^{\mathbf{V}}[a,b]$ (c) $\operatorname{curl}_h \psi^{\mathbf{V}}[a,b]$

Figure 2: $\psi^{\mathbf{V}}[a,b] \in [\mathcal{NC}_0^h(\Omega)]^2$ and its divergence and curl

3.1 Dimension of V_h

We call a square $Q \in \mathcal{T}_h$ an interior square if it has 4 interior vertices, otherwise, a boundary square. Let $\mathcal{I}_h$ be a set of all interior squares in $\mathcal{T}_h$ and denote by $\#\mathcal{I}_h$ the number of its elements. In the following lemma, $\#\mathcal{I}_h$ relates with other numbers depending on $\mathcal{T}_h$.

Lemma 3.1. *Let $\mathcal{N}(\mathbf{V}^i)$, $\mathcal{N}(Q)$ be the numbers of all interior vertices and all squares in $\mathcal{T}_h$, respectively. Then,*

$$\#\mathcal{I}_h \;=\; 2\,\mathcal{N}(\mathbf{V}^i) - \mathcal{N}(Q) + 2. \tag{16}$$

Proof. Let $\mathcal{N}(E^i)$ be the number of all interior edges in $\mathcal{T}_h$. Note the number of all boundary vertices, denoted by $\mathcal{N}(\mathbf{V}^b)$, is same as that of all boundary edges, denoted by $\mathcal{N}(E^b)$.

While we count every 4 edges a square in $\mathcal{T}_h$ to make $4\mathcal{N}(Q)$, each interior edges is done twice whereas each boundary edge is done once. That is,

$$4\mathcal{N}(Q) = 2\mathcal{N}(E^i) + \mathcal{N}(E^b). \tag{17}$$

Let k_j be the number of vertices which meet only j squares in $\mathcal{T}_h$ for $j = 1,2,3,4$. Then, $k_4 = \mathcal{N}(\mathbf{V}^i)$ and k_2 is the number of boundary vertices which are not corners, while k_1, k_3 designate those of corners of respective inner angles $90°, 270°$.

While we count every 4 vertices a square in $\mathcal{T}_h$ to make $4\mathcal{N}(Q)$, each vertex $\mathbf{V}$ is done repeatedly by its number of squares which meet $\mathbf{V}$. Thus we have,

$$4\mathcal{N}(Q) = k_1 + 2k_2 + 3k_3 + 4k_4. \tag{18}$$

From (17) subtracted by (18),

$$2\mathcal{N}(E^i) - \mathcal{N}(\mathbf{V}^b) - 4\mathcal{N}(\mathbf{V}^i) + k_1 - k_3 = 0, \tag{19}$$

since $k_1 + k_2 + k_3 = \mathcal{N}(\mathbf{V}^b) = \mathcal{N}(E^b)$.

If we paint one boundary square a boundary edge, each square which meets a corner of angle 90° is done twice by Assumption 3.1, while each corner of angle 270° has one square unpainted. It means that

$$\mathcal{N}(Q) - \#\mathcal{I}_h = \mathcal{N}(E^b) - k_1 + k_3. \tag{20}$$

From (20) added by (19), we obtain (16) through Euler's formula for simply connected domain. □

By the two color map theorem for straight lines in the plane, the squares in $\mathcal{T}_h$ are grouped into $\mathcal{R}_h$ of the red squares and $\mathcal{K}_h$ of the black ones so that no two squares of same color share an edge in $\mathcal{T}_h$, as in Figure 3.

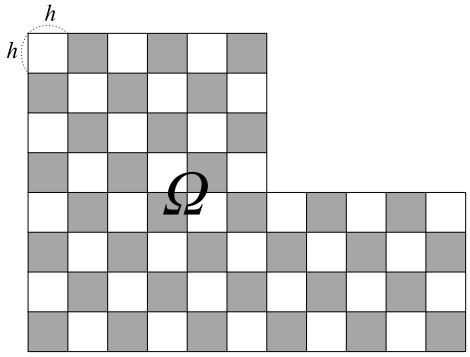

Figure 3: Red and black checkerboard in $\mathcal{T}_h$

In the following lemma, if two squares have same color, they are connected by a path which passes only squares of that color and does not meet any boundary vertices. Let

$$\mathcal{R}^\circ = \Big(\bigcup_{Q\in\mathcal{R}_h} \overline{Q} \Big) \setminus \partial\Omega, \quad \mathcal{K}^\circ = \Big(\bigcup_{Q\in\mathcal{K}_h} \overline{Q} \Big) \setminus \partial\Omega.$$

Lemma 3.2. *$\mathcal{R}^\circ$ is path-connected and so is $\mathcal{K}^\circ$.*

Proof. It is enough to prove for $\mathcal{R}^\circ$. If $\mathbf{x}, \mathbf{y} \in \mathcal{R}^\circ$, there is a path $\mathscr{P}$ in Ω joining $\mathbf{x}, \mathbf{y}$, since the open set Ω is connected. We can repair $\mathscr{P}$ into a path in $\mathcal{R}^\circ$ in the following way.

Let $\mathbf{c}_1, \mathbf{c}_2$ be two points in the path $\mathscr{P}$ which are on the boundary of a black square Q_K and the part of $\mathscr{P}$ between them, named $\mathscr{P}_{12}$, belong to the interior of Q_K. Denote by E_1, E_2, the edges of Q_K on which $\mathbf{c}_1, \mathbf{c}_2$ are, respectively. The following 3 cases are possible for E_1, E_2.

Case I. If $E_1 = E_2$, we can easily repair $\mathscr{P}_{12}$ into the segment in $\mathcal{R}^\circ$ between $\mathbf{c}_1, \mathbf{c}_2$.

Case II. Let E_1, E_2 meet at a vertex $\mathbf{V}$ of Q_K. If $\mathbf{V}$ is an interior vertex, $\mathscr{P}_{12}$ can be repaired into the 2 segments via $\mathbf{V}$ in $\mathcal{R}^\circ$ as in Figure 4-(a). When $\mathbf{V}$ is a boundary vertex, by Assumption 3.1, the other three vertices of Q_K are all interior vertices, since $\mathbf{c}_1, \mathbf{c}_2$ belong to Ω. Thus, $\mathscr{P}_{12}$ can be done into the 4 segments in $\mathcal{R}^\circ$ which do not pass $\mathbf{V}$ as in Figure 4-(b).

Case III. If E_1, E_2 are parallel, by Assumption 3.1, there are endpoints $\mathbf{V}_1, \mathbf{V}_2$ of E_1, E_2, respectively, which are interior vertices such that the segment between them is an edge of Q_K. Thus, $\mathscr{P}_{12}$ can be done into the 3 segments via $\mathbf{V}_1, \mathbf{V}_2$ in $\mathcal{R}^\circ$ as in Figure 4-(c).

□

Let $\mathcal{P}'_{0,h}(\Omega)$ be a subspace of $\mathcal{P}_{0,h}(\Omega)$ of piecewise constant functions such that

$$\mathcal{P}'_{0,h}(\Omega) \;=\; \{q_h \in \mathcal{P}_{0,h}(\Omega) \;:\; \int_{\mathcal{R}^\circ} q_h \; d\sigma = \int_{\mathcal{K}^\circ} q_h \; d\sigma = 0\}.$$

We note V_h is the kernel of the operator $\mathrm{div}_h : [\mathcal{NC}_0^h(\Omega)]^2 \longrightarrow \mathcal{P}_{0,h}(\Omega)$. The range of div_h is exactly $\mathcal{P}'_{0,h}(\Omega)$ in the following lemma.

Lemma 3.3.

$$\mathrm{div}_h\left([\mathcal{NC}_0^h(\Omega)]^2\right) = \mathcal{P}'_{0,h}(\Omega).$$

Proof. From (3), $[\mathcal{NC}_0^h(\Omega)]^2$ is spanned by $\psi^{\mathbf{V}}[1,0], \psi^{\mathbf{V}}[0,1]$ for all interior vertices $\mathbf{V}$ in $\mathcal{T}_h$. By (14), we have

$$\mathrm{div}_h \psi^{\mathbf{V}}[1,0],\ \mathrm{div}_h \psi^{\mathbf{V}}[0,1] \in \mathcal{P}'_{0,h}(\Omega).$$

It means that

$$\mathrm{div}_h\left([\mathcal{NC}_0^h(\Omega)]^2\right) \subset \mathcal{P}'_{0,h}(\Omega). \tag{21}$$

If two red squares Q_a, Q_b meet at an interior vertex $\mathbf{V}$, by (14), there is a function $\mathbf{w} \in [\mathcal{NC}_0^h(\Omega)]^2$ which is one of $(h/2)\psi^{\mathbf{V}}[\pm 1, \pm 1]$ such that

$$\mathrm{div}_h \mathbf{w}(Q_a) = 1, \quad \mathrm{div}_h \mathbf{w}(Q_b) = -1, \quad \mathrm{div}_h \mathbf{w}(Q) = 0 \text{ for all other } Q \in \mathcal{T}_h. \tag{22}$$

Let's fix one red square Q_R in $\mathcal{R}_h$. If Q is a red square in $\mathcal{R}_h$ different to Q_R, by Lemma 3.2, there is a path $\mathscr{P}$ in $\mathcal{R}^\circ$ joining two center points of Q and Q_R. Let $\mathscr{P}$ pass through a sequence of N red squares $\{Q_i\}_{i=1}^N$ in order such that

$$Q_1 = Q_R, \quad Q_N = Q, \quad Q_i \neq Q_{i+1} \text{ for } i = 1, 2, \cdots, N-1.$$

For each $i = 1, 2, \cdots, N-1$, $\overline{Q}_i \cap \overline{Q}_{i+1}$ is an interior vertex, since $\mathscr{P}$ should pass there and it dose not meet $\partial\Omega$. Thus, as in (22), there is a function $\mathbf{f}_i \in [\mathcal{NC}_0^h(\Omega)]^2$ such that

$$\mathrm{div}_h \mathbf{w}_i(Q_i) = 1, \quad \mathrm{div}_h \mathbf{w}_i(Q_{i+1}) = -1, \quad \mathrm{div}_h \mathbf{w}_i(Q) = 0 \text{ if } Q \neq Q_i, Q_{i+1}.$$

Then, setting $\mathbf{w}_h = \sum_{i=1}^{N-1} \mathbf{w}_i \in [\mathcal{NC}_0^h(\Omega)]^2$, we have

$$\mathrm{div}_h \mathbf{w}_h(Q_1) = 1, \quad \mathrm{div}_h \mathbf{w}_h(Q_N) = -1, \quad \mathrm{div}_h \mathbf{w}_h(Q) = 0 \text{ if } Q \neq Q_1, Q_N. \tag{23}$$

Since these arguments can be repeated for the black squares in $\mathcal{K}_h$, (23) means the range of div_h has at least $\mathcal{N}(Q) - 2$ linear independent piecewise constant functions. It is combined with (21) to complete the proof. □

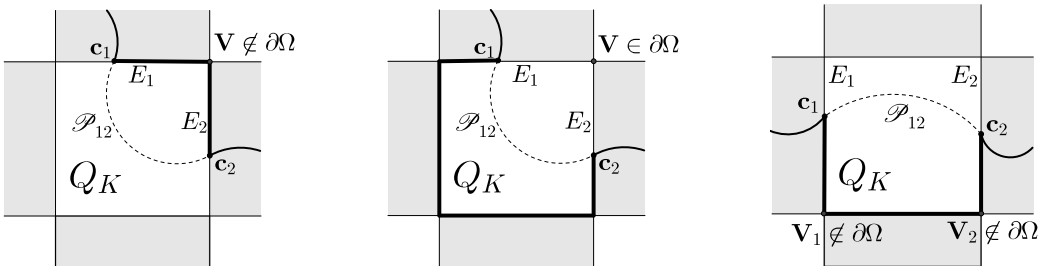

(a) $\overline{E_1} \cap \overline{E_2}$ is a vertex in Ω (b) $\overline{E_1} \cap \overline{E_2}$ is a vertex on $\partial\Omega$ (c) $\overline{E_1} \cap \overline{E_2} = \emptyset$

Figure 4: The path $\mathscr{P}_{12}$ in Q_K (dashed line) is repaired into a path in $\mathcal{R}^\circ$ (bold line)

Now, we reach at the theorem for the dimension of V_h.

Theorem 3.4. *The dimension of V_h is the number of interior squares in $\mathcal{T}_h$.*

Proof. Since V_h is the kernel of div_h, by (3) and Lemma 3.1 and 3.3, we have

$$\begin{aligned}\dim(V_h) &= \dim([\mathcal{NC}_0^h(\Omega)]^2) - \dim\left(\mathrm{div}_h\left([\mathcal{NC}_0^h(\Omega)]^2\right)\right)\\ &= 2\mathcal{N}(\mathbf{V}^i) - (\mathcal{N}(Q)-2) = \#\mathcal{I}_h.\end{aligned}$$

□

3.2 Basis for V_h

For each square Q in $\mathcal{T}_h$, denote by $\mathbf{V}^{rt}(Q), \mathbf{V}^{lt}(Q), \mathbf{V}^{lb}(Q), \mathbf{V}^{rb}(Q)$, respective vertices of Q in the right top, left top, left bottom, right bottom corners of Q as depicted in Figure 5. Let $Q^{rt}, Q^{lt}, Q^{lb}, Q^{rb}$ be squares in $\mathcal{T}_h$ whose closures intersect with $\overline{Q}$ at only $\mathbf{V}^{rt}(Q)$, $\mathbf{V}^{lt}(Q)$, $\mathbf{V}^{lb}(Q)$, $\mathbf{V}^{rb}(Q)$, respectively. If $Q \in \mathcal{T}_h$ is a boundary square, some of them are empty.

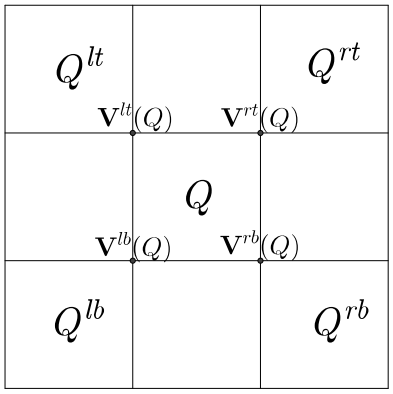

Figure 5: Name convention

For each interior square $Q \in \mathcal{I}_h$, define a locally divergence-free function $\mathbf{\Psi}_h^Q \in V_h$ by

$$\mathbf{\Psi}_h^Q = \psi^{\mathbf{V}^{rt}(Q)}[\frac{1}{2},-\frac{1}{2}] + \psi^{\mathbf{V}^{lt}(Q)}[\frac{1}{2},\frac{1}{2}] + \psi^{\mathbf{V}^{lb}(Q)}[-\frac{1}{2},\frac{1}{2}] + \psi^{\mathbf{V}^{rb}(Q)}[-\frac{1}{2},-\frac{1}{2}].$$

The nontrivial values of $\mathbf{\Psi}_h^Q$ at the midpoints of edges in $\mathcal{T}_h$ are depicted in Figure 6-(a). With (14), (15), we can easily check that $\mathrm{div}_h \mathbf{\Psi}_h^Q$ vanishes in all squares and

$$\mathrm{curl}_h \mathbf{\Psi}_h^Q = \begin{cases} -4/h & \text{in } Q,\\ 1/h & \text{in } Q^{rt}, Q^{lt}, Q^{lb}, Q^{rb},\\ 0 & \text{in other squares,}\end{cases} \tag{24}$$

as in Figure 6-(b).

Then, we are able to specify a basis for V_h in the following theorem.

Theorem 3.5. *The set $\mathcal{B} = \{\mathbf{\Psi}_h^Q \ : \ Q$ is an interior square in $\mathcal{T}_h\}$ is a basis for V_h,*

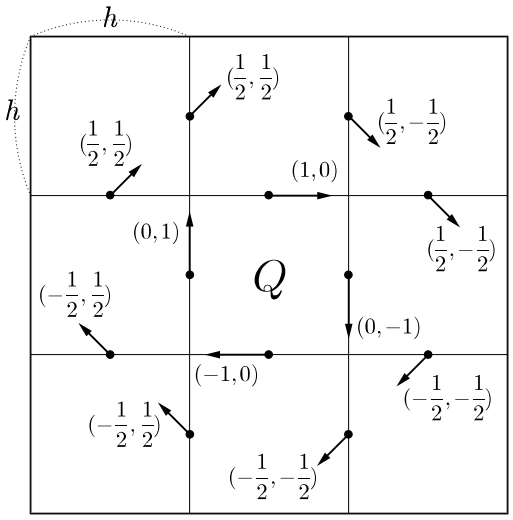

(a) Nontrivial values of $\mathbf{\Psi}_h^Q$ at midpoints

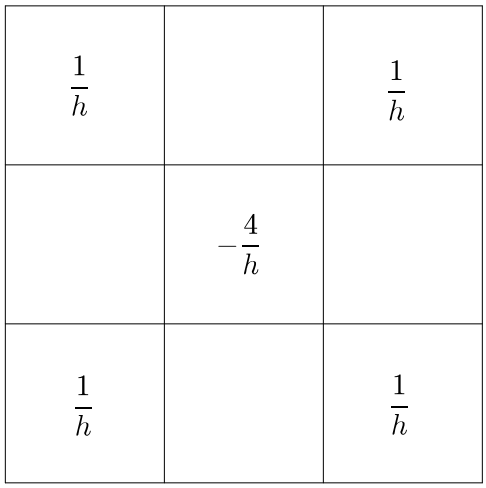

(b) Nontrivial values of $\operatorname{curl}_h \mathbf{\Psi}_h^Q$

Figure 6: Divergence-free $\mathbf{\Psi}_h^Q \in V_h$ centered at an interior square Q

Proof. By Theorem 3.4, the linear independency of $\mathcal{B}$ completes the proof. If a linear combination of functions in $\mathcal{B}$ vanish, does its discrete curl, too. Thus, it is sufficient to prove that the following set $\mathscr{F}_h$ is linearly independent,

$$\mathscr{F}_h = \{\operatorname{curl}_h \mathbf{\Psi}_h^Q \ : \ Q \text{ is an interior square in } \mathcal{T}_h\}.$$

For each square $Q \in \mathcal{T}_h$, we define a piecewise constant function $\mathbf{f}_Q \in \mathcal{P}_{0,h}(\Omega)$ by

$$\mathbf{f}_Q = \begin{cases} -4 & \text{in } Q, \\ 1 & \text{in } Q^{rt}, Q^{lt}, Q^{lb}, Q^{rb}, \\ 0 & \text{in other squares.} \end{cases} \tag{25}$$

Let N be the number of all red squares in $\mathcal{R}_h$ which are numbered as $Q_1, Q_2, \cdots, Q_N$. Regarding $\mathbf{f}_{Q_j}$ as a column vector in $\mathbb{R}^N$ for each $j = 1, 2, \cdots, N$, we have an $N \times N$ matrix M_R such that

$$M_R = [\mathbf{f}_{Q_1}, \mathbf{f}_{Q_2}, \cdots, \mathbf{f}_{Q_N}].$$

By the definition $\mathbf{f}_Q$ in (25), all columns of M_R are diagonally dominant and, if Q_j is a boundary square, the j-th column is strictly diagonally dominant. Furthermore, by Lemma 3.2, M_R is irreducible, since $M_R(i,j)$ is nonzero whenever $\overline{Q_i}, \overline{Q_j}$ intersect for $i, j = 1, 2, \cdots, N$. Thus by Taussky theorem, M_R is invertible [7]. Then, since $\mathbf{f}_Q$ is $\operatorname{curl}_h \mathbf{\Psi}_h^Q$ in (24) multiplied by h, the following set is linearly independent,

$$\mathscr{F}_h^R = \{\operatorname{curl}_h \mathbf{\Psi}_h^Q \ : \ Q \text{ is an interior red square in } \mathcal{T}_h\}.$$

Repeating same arguments for the black squares in $\mathcal{K}_h$, we have the following $\mathscr{F}_h^K$ is also linearly independent,

$$\mathscr{F}_h^K = \{\operatorname{curl}_h \mathbf{\Psi}_h^Q \ : \ Q \text{ is an interior black square in } \mathcal{T}_h\}.$$

For a red square Q and a black one Q', the supports of $\mathrm{curl}_h\,\boldsymbol{\Psi}_h^Q$ and $\mathrm{curl}_h\,\boldsymbol{\Psi}_h^{Q'}$ do not intersect. Therefore, we conclude that $\mathscr{F}_h = \mathscr{F}_h^R \cup \mathscr{F}_h^K$ is linearly independent. □

4 Application for incompressible Stokes problems

Let $(\mathbf{u}, p) \in [H_0^1(\Omega)]^2 \times L_0^2(\Omega)$ be the solution of the variational form of an incompressible Stokes equation:

$$(\nabla\mathbf{u}, \nabla\mathbf{v}) - (p, \mathrm{div}\,\mathbf{v}) + (q, \mathrm{div}\,\mathbf{u}) = (\mathbf{f}, \mathbf{v}), \quad \forall(\mathbf{v}, q) \in [H_0^1(\Omega)]^2 \times L_0^2(\Omega),$$

for a source function $\mathbf{f} \in [L^2(\Omega)]^2$.

For the finite element solution, let $(\mathbf{u}_h, p_h) \in [\mathcal{NC}_0^h(\Omega)]^2 \times \mathcal{P}'_{0,h}(\Omega)$ satisfies that

$$(\nabla\mathbf{u}_h, \nabla\mathbf{v}_h) - (p_h, \mathrm{div}\,\mathbf{v}_h) + (q_h, \mathrm{div}\,\mathbf{u}_h) = (\mathbf{f}, \mathbf{v}_h), \quad \forall(\mathbf{v}_h, q_h) \in [\mathcal{NC}_0^h(\Omega)]^2 \times \mathcal{P}'_{0,h}(\Omega). \quad (26)$$

If $\mathbf{u} \in [H^2(\Omega)]^2, p \in H^1(\Omega)$, the following error estimate holds

$$|\mathbf{u} - \mathbf{u}_h|_{1,h} + \|p - p_h\|_0 \le C_\Omega h(|\mathbf{u}|_2 + |p|_1), \quad (27)$$

since $[\mathcal{NC}_0^h(\Omega)]^2 \times \mathcal{P}'_{0,h}(\Omega)$ satisfies the inf-sup condition [9].

In an alternate way to get $(\mathbf{u}_h, p_h) \in [\mathcal{NC}_0^h(\Omega)]^2 \times \mathcal{P}'_{0,h}(\Omega)$ in (26), we can solve an elliptic problem for velocity and apply an explicit method for pressure as in next two subsections.

4.1 Elliptic problem for velocity

The discrete velocity $\mathbf{u}_h$ in (26) satisfies that

$$(q_h, \mathrm{div}\,\mathbf{u}_h) = 0, \quad \text{for all } q_h \in \mathcal{P}'_{0,h}(\Omega).$$

Since there exists $q_h \in \mathcal{P}'_{0,h}(\Omega)$ such that $q_h = \mathrm{div}\,\mathbf{u}_h$ from (14), we have

$$\mathbf{u}_h \in V_h,$$

for the locally divergence-free finite element space V_h in (13). Thus, to get $\mathbf{u}_h$ in (26), we can solve the following elliptic problem for velocity:

$$(\nabla\mathbf{u}_h, \nabla\mathbf{v}_h) = (\mathbf{f}, \mathbf{v}_h), \quad \forall\mathbf{v}_h \in V_h, \quad (28)$$

which smaller than the problem (26).

We note, since the norm is decomposed in Lemma 2.2, so is the inner product as

$$(\nabla\mathbf{v}_h, \nabla\mathbf{w}_h) = (\mathrm{div}_h\,\mathbf{v}_h, \mathrm{div}_h\,\mathbf{w}_h) + (\mathrm{curl}_h\,\mathbf{v}_h, \mathrm{curl}_h\,\mathbf{w}_h), \quad \forall\mathbf{v}_h, \mathbf{w}_h \in [\mathcal{NC}_0^h(\Omega)]^2.$$

The above means

$$(\nabla\mathbf{v}_h, \nabla\mathbf{w}_h) = (\mathrm{curl}_h\,\mathbf{v}_h, \mathrm{curl}_h\,\mathbf{w}_h), \quad \forall\mathbf{v}_h, \mathbf{w}_h \in V_h.$$

Thus, the problem (28) is equivalent to

$$(\mathrm{curl}_h\,\mathbf{u}_h, \mathrm{curl}_h\,\mathbf{v}_h) = (\mathbf{f}, \mathbf{v}_h), \quad \forall\mathbf{v}_h \in V_h. \quad (29)$$

Suggested in Theorem 3.5, a basis $\mathcal{B}$ for V_h consists of $\mathbf{\Psi}_h^Q$ for all interior square $Q \in \mathcal{T}_h$. For an interior square Q, although the support of the basis function $\mathbf{\Psi}_h^Q$ in V_h consists of 9 squares, that of $\mathrm{curl}_h \mathbf{\Psi}_h^Q$ is 5 squares as in Figure 6. If we assume $h = 1$ for simplicity, as in Figure 7, 8, 9, 10, we have

$$(\nabla\mathbf{\Psi}_h^Q, \nabla\mathbf{\Psi}_h^{Q'}) = \begin{cases} 20 & \text{if } Q = Q', \\ 2 & \text{if supports of } \nabla\mathbf{\Psi}_h^Q, \nabla\mathbf{\Psi}_h^{Q'} \text{ meet at 3 squares}, \\ -8 & \text{if supports of } \nabla\mathbf{\Psi}_h^Q, \nabla\mathbf{\Psi}_h^{Q'} \text{ meet at 4 squares}, \\ 1 & \text{if supports of } \nabla\mathbf{\Psi}_h^Q, \nabla\mathbf{\Psi}_h^{Q'} \text{ meet at 1 square}. \end{cases}$$

Besides, if Q is a red square, the support of $\mathrm{curl}_h \mathbf{\Psi}_h^Q$ lies in 5 red squares, and vice versa

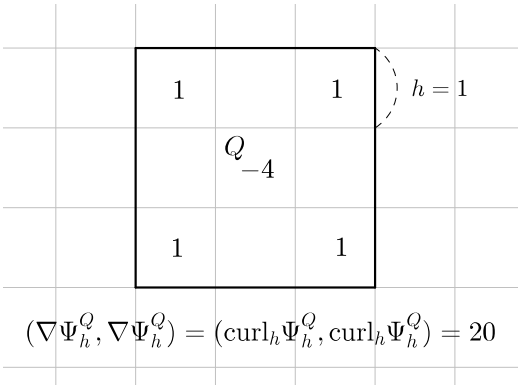

Figure 7: Inner product $(\nabla\mathbf{\Psi}_h^Q, \nabla\mathbf{\Psi}_h^Q)$ when $h = 1$

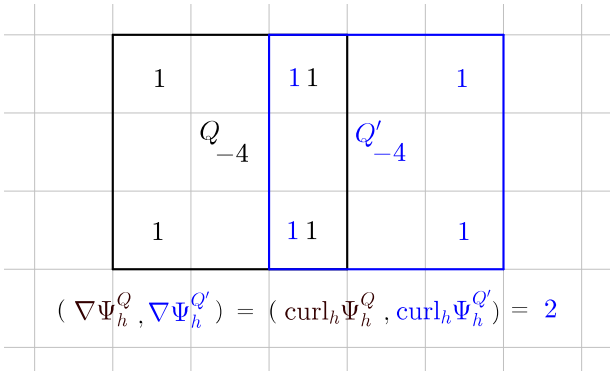

Figure 8: Inner product of $\nabla\mathbf{\Psi}_h^Q, \nabla\mathbf{\Psi}_h^{Q'}$ when their supports meet at 3 squares

for a black square. Thus, their supports do not meet each other as in Figure 11. It means the following lemma.

Lemma 4.1. *For each interior red square Q_R and black square Q_K,*

$$(\nabla\mathbf{\Psi}_h^{Q_R}, \nabla\mathbf{\Psi}_h^{Q_K}) = 0.$$

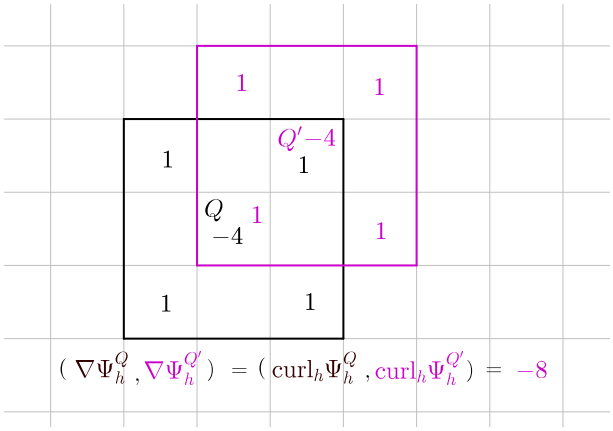

Figure 9: Inner product of $\nabla\boldsymbol{\Psi}_h^Q, \nabla\boldsymbol{\Psi}_h^{Q'}$ when their supports meet at 4 squares

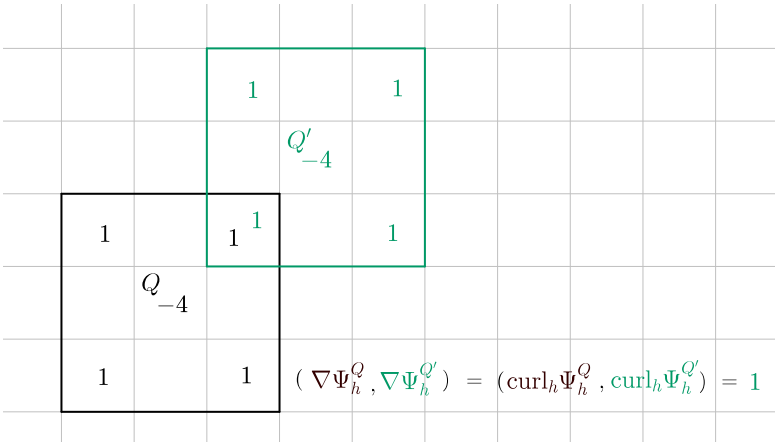

Figure 10: Inner product of $\nabla\boldsymbol{\Psi}_h^Q, \nabla\boldsymbol{\Psi}_h^{Q'}$ when their supports meet at 1 square

As a result, when we implement the finite element method to solve (28) with the basis $\mathcal{B}$ for V_h, the inner products $(\nabla\boldsymbol{\Psi}_h^Q, \nabla\boldsymbol{\Psi}_h^{Q'})$ vanish except at most 13 Q' for a fixed interior square $Q \in \mathcal{T}_h$, as in Figure 12. Thus the sparsity of the system of linear equations is not as large as expected from the support of $\boldsymbol{\Psi}_h^Q$.

Furthermore, by Lemma 4.1, the system of linear equations to solve (28) with the basis $\mathcal{B}$ for V_h can be split into two smaller ones with the following $\mathcal{B}_R, \mathcal{B}_K$ for red and black squares, respectively,

$$\begin{aligned} \mathcal{B}_R &= \{\boldsymbol{\Psi}_h^Q \ : \ Q \text{ is an interior red square in } \mathcal{T}_h\}, \\ \mathcal{B}_K &= \{\boldsymbol{\Psi}_h^Q \ : \ Q \text{ is an interior black square in } \mathcal{T}_h\}. \end{aligned} \tag{30}$$

4.2 Explicit method for pressure recovery

We will find the discrete pressure $p_h \in \mathcal{P}'_{0,h}(\Omega)$ in (26) by an explicit method using the a priori obtained discrete velocity $\mathbf{u}_h \in V_h$ in (26) through the elliptic problem (28).

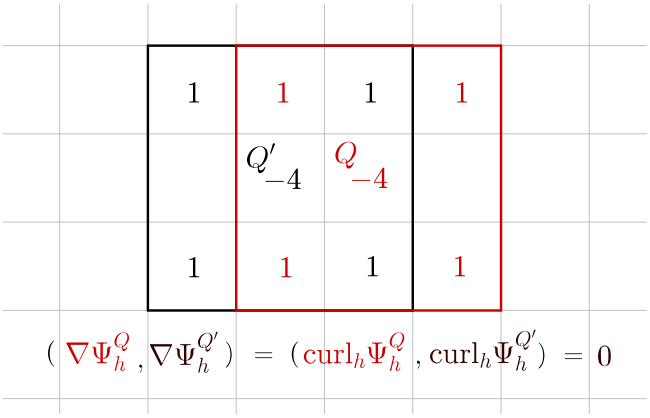

Figure 11: $\mathrm{curl}_h \boldsymbol{\Psi}_h^Q$ for red square Q, $\mathrm{curl}_h \boldsymbol{\Psi}_h^{Q'}$ for black square Q' : They do not meet.

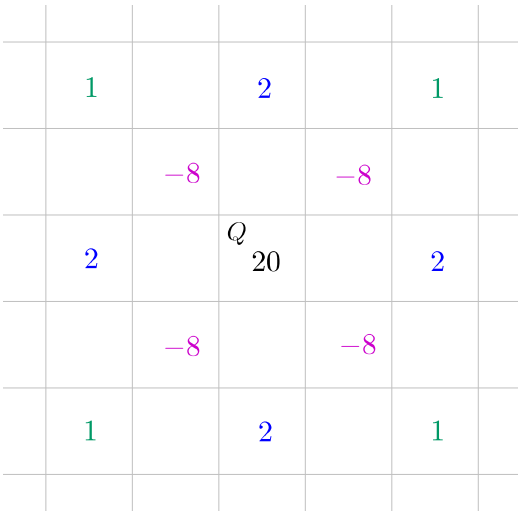

Figure 12: 13 nonzero $(\nabla\boldsymbol{\Psi}_h^Q, \nabla\boldsymbol{\Psi}_h^{Q'})$ for fixed Q

Let's consider the problem (P): Find $a_h \in \mathcal{P}'_{0,h}(\Omega)$ such that

$$(a_h, \mathrm{div}_h\, \mathbf{v}_h) = (\nabla \mathbf{u}_h, \nabla \mathbf{v}_h) - (\mathbf{f}, \mathbf{v}_h), \quad \forall \mathbf{v}_h \in [\mathcal{NC}_0^h(\Omega)]^2.$$

By Lemma 3.3, $p_h \in \mathcal{P}'_{0,h}(\Omega)$ in (26) is the unique solution of the problem (P).

Define two checkerboard functions $\chi_R, \chi_K \in \mathcal{P}_{0,h}(\Omega)$ by

$$\chi_R(Q) = \begin{cases} 1, & \text{if } Q \text{ is a red square,} \\ 0, & \text{if } Q \text{ is a black square,} \end{cases} \qquad \chi_K(Q) = \begin{cases} 0, & \text{if } Q \text{ is a red square,} \\ 1, & \text{if } Q \text{ is a black square.} \end{cases}$$

We have, for all $\mathbf{v}_h \in [\mathcal{NC}_0^h(\Omega)]^2$,

$$(\chi_R, \mathrm{div}_h\, \mathbf{v}_h) = (\chi_K, \mathrm{div}_h\, \mathbf{v}_h) = (\chi_R, \chi_K) = 0. \tag{31}$$

Let's fix a red square Q_R, a black one Q_K and define $\hat{p_h} \in \mathcal{P}_{0,h}(\Omega)$ by

$$\hat{p_h} = p_h - C_R\chi_R - C_k\chi_K,$$

for two constants $C_R = p_h(Q_R), C_K = p_h(Q_K)$. Then, by (31), $\hat{p_h} \in \mathcal{P}_{0,h}(\Omega)$ satisfies

$$\begin{gathered}(\hat{p_h}, \operatorname{div}_h \mathbf{v}_h) = (\nabla \mathbf{u}_h, \nabla \mathbf{v}_h) - (\mathbf{f}, \mathbf{v}_h), \quad \forall \mathbf{v}_h \in [\mathcal{NC}_0^h(\Omega)]^2, \\ \hat{p_h}(Q_R) = \hat{p_h}(Q_K) = 0.\end{gathered} \tag{32}$$

We will find $\hat{p_h}$ satisfying (32) by an explicit method. If other red square Q'_R meets with Q_R at an interior vertex, there is a function $\mathbf{v}_h \in [\mathcal{NC}_0^h(\Omega)]^2$ as in (22) such that

$$\operatorname{div}_h \mathbf{v}_h(Q'_R) = 1, \quad \operatorname{div}_h \mathbf{v}_h(Q_R) = -1, \quad \operatorname{div}_h \mathbf{v}_h(Q) = 0 \text{ for all other } Q \in \mathcal{T}_h. \tag{33}$$

Then, from (32) and (33), $\hat{p_h}$ at Q'_R is determined by

$$\int_{Q'_R} \hat{p_h} \, d\sigma = \int_{Q_R} \hat{p_h} \, d\sigma + (\nabla \mathbf{u}_h, \nabla \mathbf{v}_h) - (\mathbf{f}, \mathbf{v}_h).$$

In this manner, we can find $\hat{p_h}$ at all red squares by an explicit telescoping methods using such simple $\operatorname{div}_h \mathbf{v}_h$ as in (33), since all red ones are connected through interior vertices as in the proof of Theorem 3.4. Applying the same telescoping methods for the black squares, we get a piecewise constant function $\hat{p_h} \in \mathcal{P}_{0,h}(\Omega)$ satisfying (32).

Then, we can obtain the unique solution $p_h \in \mathcal{P}'_{0,h}(\Omega)$ of the problem (P) so that

$$p_h = \hat{p_h} - D_R \chi_R - D_K \chi_K,$$

where D_R and D_K are constants such that

$$D_R = \frac{(\hat{p_h}, \chi_R)}{(\chi_R, \chi_R)}, \quad D_K = \frac{(\hat{p_h}, \chi_K)}{(\chi_K, \chi_K)}.$$

5 Numerical results

We chose the velocity $\mathbf{v}$ and pressure p on $\Omega = [0,1]^2$ for numerical tests, as

$$\mathbf{u} = (\phi_y, -\phi_x), \quad p = \sin(4\pi x) e^{\pi y},$$

where ϕ is the stream function such that

$$\phi(x,y) = \sin(2\pi x) \sin(3\pi y)(x^3 - x)(y^2 - y).$$

The discrete velocity $\mathbf{u}_h$ is the sum of two solutions of the problems (29) in V_h with two separable bases $\mathcal{B}_R$ and $\mathcal{B}_K$ in (30) for red and black squares, respectively.

The cardinalities of $\mathcal{B}_R$ and $\mathcal{B}_K$ are same and much smaller than the dimension of the entire space $[\mathcal{NC}_0^h(\Omega)]^2 \times \mathcal{P}'_{0,h}(\Omega)$ as in Table 1. Each system of linear equations with $\mathcal{B}_R$ and $\mathcal{B}_K$ was solved by a direct method based on the Cholesky decomposition.

After solving $\mathbf{u}_h$, we obtained the discrete pressure p_h by the explicit method suggested in subsection 4.2. The numerical results in Table 2 show the optimal order of error decay expected in (27).

References

[1] S. Brenner, F. Li and L. Sung, A locally divergence-free nonconforming finite element method for the reduced time-harmonic Maxwell equations, Math. Comp., 76 (2007), 573-595

[2] F. Brezzi and M. Fortin, Mixed and hybrid finite element methods, Springer-Verlag, New York, 1991

[3] B. Cockburn, F. Li and C. Shu, Locally divergence-free discontinuous Galerkin methods for the Maxwell equations, J. Comput. Phys., 194 (2004), 588-610

[4] B. Cockburn, G. Kanschat and D. Schötzau, A note on discontinuous Galerkin divergence-free solutions of the Navier-Stokes equations, J. Sci. Comput., 31 (2007), 61-73

[5] V. Girault and P. A. Raviart, Finite element methods for the Navier-Stokes equations: Theory and Algorithms, Springer-Verlag, New York, 1986

[6] F. Hecht, Construction d'une base de fonctions P_1 non conforme á divergence nulle dans $\mathbb{R}^3$, RAIRO Anal. Numér., 15 (1981), 119-150

[7] R. Horn and C. Johnson, Matrix analysis, Cambridge University Press, New York, 1985

[8] Y. Huang and S. Zhang, A lowest order divergence-free finite element on rectangular grids, Front. Math. China, 6 (2011), 253-270

[9] S. Kim, J. Yim and D. Sheen, Stable cheapest nonconforming finite elements for the Stokes equations, J. Comp. Appl. Math., 299 (2016), 2-14, doi:10.1016/j.cam.2015.06.021

[10] C. Park, A Study on Locking phenomena in finite element methods, Ph.D. thesis, Department of mathematics, Seoul National University, Seoul, Korea, 2002

[11] C. Park and D. Sheen, P_1-nonconforming quadrilateral finite element methods for second-order elliptic problems, SIAM J. Numer. Anal., 41 (2003), 624-640

[12] M. Powell and M. Sabin, Piecewise quadratic approximations on triangles, ACM Trans. Math. Software, 3 (1977), 316-325

mesh	$\dim(\text{Span } \mathcal{B}_R) = \dim(\text{Span } \mathcal{B}_K)$	$\dim\left([\mathcal{NC}_0^h(\Omega)]^2 \times \mathcal{P}'_{0,h}(\Omega)\right)$
8 x 8	18	160
16 x 16	98	704
32 x 32	450	2,944
64 x 64	1,922	12,032
128 x 128	7,938	48,640
256 x 256	32,258	195,584
512 x 512	130,050	784,384
1024 x 1024	522,242	3,141,632

Table 1: Dimensions of Span $\mathcal{B}_R$, Span $\mathcal{B}_K$ and $[\mathcal{NC}_0^h(\Omega)]^2 \times \mathcal{P}'_{0,h}(\Omega)$

mesh	$\|\mathbf{u}-\mathbf{u}_h\|_0$		$\|\mathbf{u}-\mathbf{u}_h\|_{1,h}$		$\|p-p_h\|_0$	
	value	order	value	order	value	order
8 x 8	5.6091E-2		2.1164E+0		2.9913E+0	
16 x 16	1.3451E-2	2.0601	1.0774E+0	0.9740	1.5145E+0	0.9819
32 x 32	3.3342E-3	2.0123	5.4115E-1	0.9935	7.6081E-1	0.9933
64 x 64	8.3187E-4	2.0029	2.7088E-1	0.9984	3.8088E-1	0.9982
128 x 128	2.0786E-4	2.0007	1.3548E-1	0.9996	1.9050E-1	0.9995
256 x 256	5.1959E-5	2.0002	6.7743E-2	0.9999	9.5257E-2	0.9999
512 x 512	1.2990E-5	2.0000	3.3872E-2	1.0000	4.7630E-2	1.0000
1024 x 1024	3.2497E-6	1.9990	1.6936E-2	1.0000	2.3815E-2	1.0000

Table 2: Error table for the divergence-free method

[13] F. Thomasset, Implementation of Finite Element Methods for Navier-Stokes Equations, Springer-Verlag, New York-Berlin, 1981

[14] S. Zhang, A family of $Q_{k+1,k} \times Q_{k,k+1}$ divergence-free finite elements on rectangular grids, SIAM J. Numer. Anal., 47 (2009), 2090-2107